



Vitamin D₃ transactivates the zinc and manganese transporter SLC30A10 via the Vitamin D receptor



Tatiana Claro da Silva, Christian Hiller, Zhibo Gai, Gerd A. Kullak-Ublick*

Department of Clinical Pharmacology and Toxicology, University Hospital Zurich, University of Zurich, Switzerland

ARTICLE INFO

Article history:

Received 28 July 2015

Received in revised form 15 March 2016

Accepted 13 April 2016

Available online 20 April 2016

Keywords:

Vitamin D

SLC30A10

Zinc

Manganese

VDRE

Iron

ABSTRACT

Vitamin D₃ regulates genes critical for human health and its deficiency is associated with an increased risk for osteoporosis, cancer, diabetes, multiple sclerosis, hypertension, inflammatory and immunological diseases. To study the impact of vitamin D₃ on genes relevant for the transport and metabolism of nutrients and drugs, we employed next-generation sequencing (NGS) and analyzed global gene expression of the human-derived Caco-2 cell line treated with 500 nM vitamin D₃. Genes involved in neuropeptide signaling, inflammation, cell adhesion and morphogenesis were differentially expressed. Notably, genes implicated in zinc, manganese and iron homeostasis were largely increased by vitamin D₃ treatment. An ~10-fold increase in ceruloplasmin and ~4-fold increase in haptoglobin gene expression suggested a possible association between vitamin D and iron homeostasis. SLC30A10, the gene encoding the zinc and manganese transporter ZnT10, was the chiefly affected transporter, with ~15-fold increase in expression. SLC30A10 is critical for zinc and manganese homeostasis and mutations in this gene, resulting in impaired ZnT10 function or expression, cause manganese intoxication, with Parkinson-like symptoms. Our NGS results were validated by real-time PCR in Caco-2 cells, as well as in duodenal biopsies taken from healthy human subjects treated with 0.5 µg vitamin D₃ daily for 10 days. In addition to increasing gene expression of SLC30A10 and the positive control TRPV6, vitamin D₃ also increased ZnT10 protein expression, as indicated by Western blot and cytofluorescence. In silico identification of potential vitamin D responsive elements (VDREs) in the 5'-flanking region of the SLC30A10 promoter and dual-luciferase reporter assay showed enhanced promoter activity in the presence of vitamin D receptor (VDR) and retinoid X receptor (RXR) constructs, as well as vitamin D₃, but not when one of these factors was absent. Electrophoretic mobility shift assay (EMSA) and competition EMSA revealed binding of select sequences, namely, nt -1623/-1588 and nt -1758/-1723 relative to the transcription start site, to VDR-containing nuclear extracts. In conclusion, we have shown that vitamin D₃ transactivates the SLC30A10 gene in a VDR-dependent manner, resulting in increased ZnT10 protein expression. Because SLC30A10 is highly expressed in the small intestine, it is possible that the control of zinc and manganese systemic levels is regulated by vitamin D₃ in the intestine. Zinc, manganese and vitamin D are important for bone metabolism and brain health. Future examination of a possible role for supplementation or chelation of zinc and manganese, alongside vitamin D₃ administration, will further our understanding of its potential benefit in the treatment of specific illnesses, such as osteoporosis and Parkinson's disease. © 2016 The Author(s). Published by Elsevier Ltd. This is an open access article under the CC BY-NC-ND license (<http://creativecommons.org/licenses/by-nc-nd/4.0/>).

1. Introduction

Vitamin D is involved in several physiological processes, ranging from inflammation to glucose homeostasis and blood pressure, to name a few [1]. Deficiency in vitamin D is pandemic [2]

and is correlated with asthma, diabetes, cancer and neuropsychiatric disorders [3]. While vitamin D can be obtained from fatty fish and fortified foods, its main natural source is the provitamin D, 7-dehydrocholesterol, found in the skin. Photochemical conversion of 7-dehydrocholesterol, initiated by skin exposure to UV light, is the first step in the production of the biologically active vitamin D hormone. The product of this conversion is carried to the liver, where it is transformed into 25-hydroxyvitamin D (25OHD), which is then oxidized, predominantly in the kidney, to form the active hormone 1,25-dihydroxyvitamin D (1,25D), or vitamin D₃. To exert its gene regulatory effect, vitamin D₃ binds to the vitamin D

* Corresponding author at: Department of Clinical Pharmacology and Toxicology, University Hospital Zurich, Rämistrasse 100, CH-8091 Zurich, Switzerland.

E-mail addresses: taticlaro@yahoo.com (T. Claro da Silva),

christian.hiller@usz.ch (C. Hiller), zhibo.gai@usz.ch (Z. Gai), gerd.kullak@usz.ch (G.A. Kullak-Ublick).

receptor (VDR), which in turn dimerizes with the retinoid-X receptor (RXR) and binds vitamin D response elements (VDREs) in the promoter region of target genes, culminating in transcriptional activation or repression. Genes thus regulated include the calcium channel transient receptor potential vanilloid 6 (TRPV6) [4], the vitamin D₃ 24-hydroxylase CYP24A1 [5] and the organic anion transporting polypeptide 1A2 (SLC01A2; OATP1A2) [6]. Our present data shows that treatment of human derived Caco-2 cells with vitamin D₃ altered gene expression of these and other genes relevant for a variety of physiological processes, including drug metabolism and transport. Iron homeostasis was among the most affected processes and may suggest that a correlation between vitamin D₃ levels and iron regulation exists at the molecular level. Our results also indicate that expression of the SLC30A10 gene, as well as its encoded protein, the zinc (Zn) and manganese (Mn) transporter ZnT10, are augmented by vitamin D₃ treatment in Caco-2 cells. SLC30A10 mRNA is predominantly expressed in human liver, brain, testis and small intestine [7,8]. Missense and nonsense mutations in this gene, impairing ZnT10 expression or cell surface trafficking, cause manganism – a Parkinson-like autosomal recessive disease characterized by dystonia, hypermanganesemia, steatosis, cirrhosis and polycythemia [9]. By means of its Mn efflux action, ZnT10 protects the CNS from manganese toxicity and ZnT10 dysfunction leads to accumulation of Mn in the liver and nervous system [10], even in patients without prior history of environmental exposure to high Mn levels [8]. Zn and Mn are classified as trace elements or micronutrients because they are essential for human health albeit needed in small quantities, whereas at high concentrations, they exhibit toxic effects [11]. It is interesting to note that, in addition to the renowned vitamin D and calcium contributions, Zn and Mn are crucial for bone metabolism [12]. They are absorbed from the intestine [10], where the gene encoding ZnT10, SLC30A10, is highly expressed at the mRNA level [7] and where the VDR is also abundant [13]. Because our results indicate that vitamin D₃ induces SLC30A10 gene and protein expression, it is likely that the control of Zn and Mn systemic levels begins in the intestine and is dependent on the vitamin D nutritional status.

2. Material and methods

2.1. Cell culture

The human-derived Caco-2 cell line (LGC Promochem, Molsheim, Switzerland) was cultured in Dulbecco's modified Eagle's medium (ThermoFisher) containing 10% fetal bovine serum (Chemie Brunschwig) and 1000 U/mL and 1000 g/mL penicillin and streptomycin, respectively (Invitrogen, Carlsbad, CA). Cells were maintained at 37 °C, in a humidified atmosphere containing 5% CO₂.

2.2. Next generation sequencing (NGS)

Caco-2 cells were treated with 500 nM 1,25 dihydroxyvitamin D₃ (vitamin D₃) or vehicle (ethanol; EtOH) for 8 h, 24 h, 48 h and 72 h. Cells were harvested in TRIzol[®] and total RNA was isolated using the guanidinium thiocyanate-phenol-chloroform extraction method. At the Functional Genomics Center Zurich, the isolated RNA was reverse-transcribed and amplified by PCR, then next-generation sequencing on the Illumina HiSeq 2000 (TruSeq SBS Kit v3-HS (Illumina)) was performed. Changes were considered significant when p value ≤ 0.05 and the increase or decrease in expression was at least 40% (log₂ ratio ≥ 0.5 or ≤ -0.75) compared to the vehicle control (EtOH). MetaCore online service (Thomson Reuters) was employed for gene ontology and network analysis. Select genes altered by vitamin D₃ in the NGS data were chosen for further investigation.

2.3. Vitamin D₃ administration in healthy human volunteers

In a prospective single-center study performed at the University of Zurich, six female and four male healthy volunteers (aged 24–29 years, mean 26 years, median 26 years) self-administered 1,25 dihydroxyvitamin D₃ (Rocaltrol[®]) 0.5 µg per day for 10 days. Duodenal biopsies were collected by gastroscopy before ("FIRST" gastroscopy) and after ("SECOND" gastroscopy) the onset of Rocaltrol[®] administration and were immediately frozen in liquid nitrogen. Subsequently, biopsies were analyzed by real-time PCR (RT-PCR) as described in the next Section (2.4), to confirm gene changes observed in the NGS data. This study was performed in conformity with the Good Clinical Practice guideline ICH E6 after having been approved by the ethical committee of the Canton of Zurich (license number 2012-0051) and registered at clinicaltrials.gov (NCT01856348). All volunteers signed the informed consent.

2.4. Analysis of duodenal biopsies and Caco-2 cells by real-time PCR

Extraction of RNA from duodenal biopsies and Caco-2 cells was performed using the Nucleospin miRNA kit (Macherey-Nagel, Inc.). Prior to processing, duodenal biopsies were homogenized with a 1.5 mL pestle (VWR cat. # 47747-358, European Article # 431-0094) following recommendations from the Nucleospin miRNA kit's manufacturer. After tissue homogenization, biopsies and Caco-2 cells were processed similarly. Extracted RNA was subsequently evaluated by RT-PCR for selected drug and nutrient transporters, using TaqMan probes (ThermoFisher). Data obtained was normalized to the housekeeping genes villin (biopsies) or beta-actin (Caco-2 cells).

2.5. Isolation of a total membrane fraction from cultured Caco-2 cells

Caco-2 cells grown in 10 mm petri dishes were treated with 500 nM 1,25 dihydroxyvitamin D₃ (vitamin D₃) or vehicle (ethanol; EtOH) for 72 h with refreshment of vitamin D₃ or EtOH every 24 h. The following procedure was performed on ice. Briefly, cells were washed 3x in 10 mL of 0.9% (w/v) NaCl solution, followed by 1x addition of 10 mL 250 mM sucrose solution. Subsequently, 3 mL ice-cold 5 mM sucrose solution, containing 5 mM phenylmethanesulfonyl fluoride (PMSF; freshly added from a 200 mM stock in EtOH) and 1 mg/ml antipain/leupeptin (freshly added from 1 mg/ml stock each) was added and cells were scraped with a rubber policeman, then transferred to a tight fitting glass-TEFLON potter on ice and homogenized with 20 strokes at full speed. Homogenate was then centrifuged at 4 °C for 10 min at 2950 rpm (900g_{av}) in a Sorvall SS34 rotor and the supernatant was carefully removed and centrifuged at 4 °C for 20 min at 9600 rpm (8500g_{av}) in a Sorvall SS34 rotor. Next, the resulting supernatant was carefully removed and centrifuged at 4 °C for 1 h, at 38,200 rpm (100,000g_{av}) in a TFT 65.13 rotor or at 36,400 rpm (100,000g_{av}) in a TFT 70.38 rotor. After complete removal of the supernatant, ~500 µL of a 250 mM sucrose solution containing protease inhibitors was added to the precipitate and this suspension was homogenized with a 1 mL syringe and a thin needle. Approximately 10–20 µL of the resulting solution was separated for protein determination and the remaining membrane fraction was stored in liquid nitrogen until use.

2.6. Western blotting

Lysates containing 20 µg of protein from the isolated Caco-2 membrane fraction described above were separated by SDS-PAGE and blotted on polyvinylidene difluoride membranes (Millipore). Membranes were blocked with TBS containing 0.1% Tween 20 (TBST) and 3% BSA, for 1 h, at room temperature. The

primary antibodies rabbit anti-SLC30A10 (Sigma-Aldrich, HPA017989) and the plasma membrane control goat anti-Na + K + ATPase (Santa Cruz, sc-16041) were then incubated overnight at 4 °C. After washing the membranes with TBST, blots were treated with horseradish peroxidase conjugated secondary antibodies at room temperature for 1 h, washed again with TBST and developed using the ECL Plus detection system (Amersham Biosciences, Little Chalfont, UK).

2.7. Cytofluorescence

Caco-2 cells grown on 3 mm slides were treated with 500 nM 1,25 dihydroxyvitamin D₃ (vitamin D₃) or vehicle (ethanol; EtOH) for 72 h with refreshment of vitamin D₃ or EtOH every 24 h. After treatment, cells were washed with cold PBS, fixed in 4% paraformaldehyde, and treated with 0.1% Triton X in PBS for 15 min and with 0.1% Tween-20 in 1% BSA/PBS for 30 min. Then, cells were incubated with rabbit anti-SLC30A10 (Sigma-Aldrich, HPA017989) antibody at 4 °C overnight. Cells were then washed and incubated with secondary antibody for 1 h at room temperature, in the dark. After being washed, cells were counterstained with 4'-6-diamidino-2-phenylindole (DAPI; Vector Laboratories) and slides were mounted and visualized under a fluorescent microscope (Leica DMI6000B).

2.8. Identification of VDREs in silico and DNA constructs

In silico analysis of the 5'-flanking region enclosing ~3.6 kb upstream the transcription start site (TSS) and ~211 bp downstream the ATG start codon, *i.e.*, -3622/+211, of the

SLC30A10 promoter, revealed several conjectural vitamin D response elements (VDREs). This analysis was performed with the online transcription factor binding site prediction tools PROMO [14,15] and MatInspector [16,17], as well as by visual inspection of canonical sites, based on sequences described in Toell et al. [18]. This ~3.8 kb region was then synthesized, cloned and subcloned into the pGL3 basic luciferase reporter vector (Promega) using GeneArt services, for subsequent dual-luciferase reporter assay. Briefly, the synthesized fragment was cloned into the pMK vector, carrying a kanamycin resistance gene, and was then subcloned into the Nhe/XhoI-digested pGL3 basic vector. Dual-luciferase reporter assay was carried out as described below (Section 2.9). *In silico* predicted VDREs were also incorporated in the design of oligonucleotides used in electrophoretic mobility shift assay (EMSA), as described in Section 2.10.

2.9. Dual-Luciferase reporter assay

Caco-2 cells were seeded in 48-well plates and transiently transfected at a confluence of approximately 80%, on the next day. The transfection agent Fugene HD (Promega) was used to deliver DNA to the cells, in a transfection mixture containing 400 ng of the pGL3 basic constructs (Section 2.8) and 200 ng of VDR and/or RXR expression plasmid in pCMX. The pCMX-VDR and pCMX-RXR plasmids were kindly donated by Dr. David Mangelsdorf (University of Texas Southwestern Medical Center, Dallas, TX). In each well, 100 ng of phRG-TK Renilla reniformis luciferase reporter plasmid (Promega) was co-transfected to account for variations in transfection efficiency. An appropriate volume of 1 α ,25-dihydroxyvitamin D₃ (Sigma-Aldrich) or its vehicle EtOH, was added to each

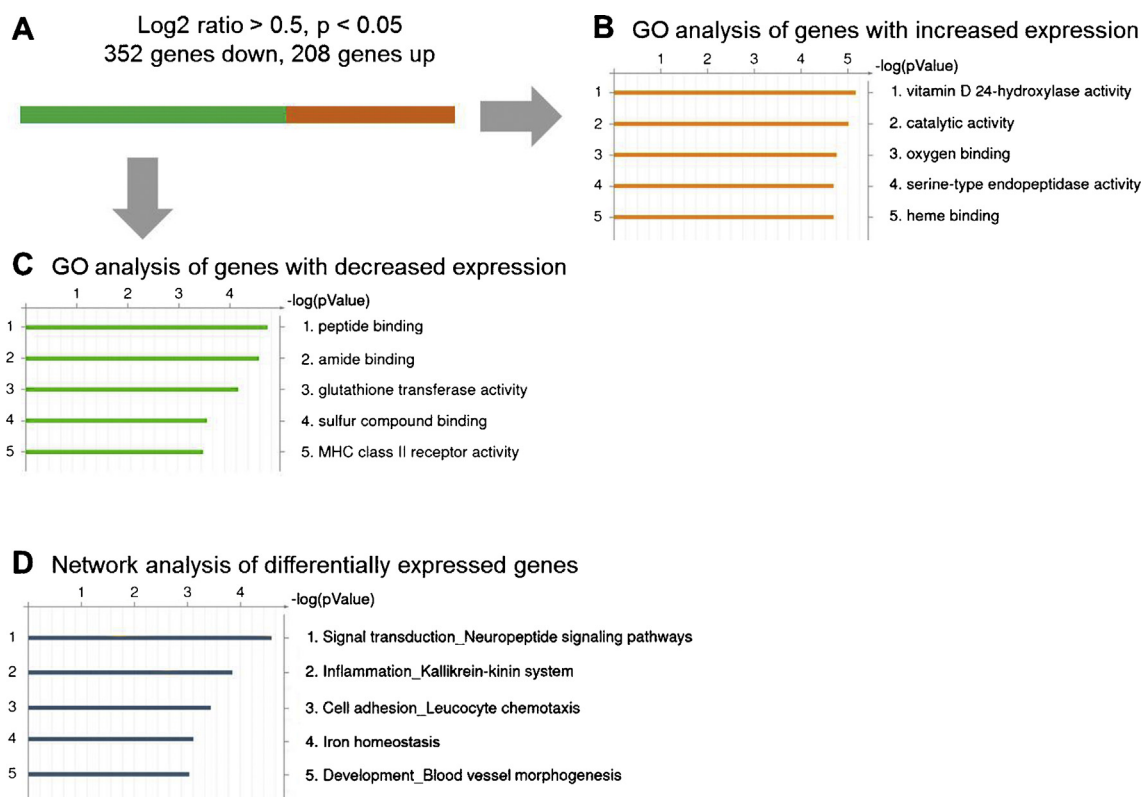


Fig. 1. Effect of vitamin D treatment on gene expression patterns in Caco-2 cells. (A) Summary of differentially expressed genes between Vit. D treatment for 24 h and vehicle control (EtOH). Genes that are differentially increased or decreased after Vit D treatment are indicated by orange and green bars, respectively. Cut off 1.4-fold, p < 0.05. Of all 560 genes with significantly changed expression after Vit. D treatment for 24 h, 208 genes are increased and 352 genes are reduced. (B) Gene ontology (GO) analysis of genes with a ≥ 1.4 fold increased expression (orange bars). (C) GO analysis of genes with a ≥ 1.4 fold decreased expression (green bars). (D) Network analysis of genes with a change of expression of ≥ 1.4 fold across treatment groups. The top 5 results are listed. All analyses were performed with the MetaCore online software (Thomson Reuters). (For interpretation of the references to colour in this figure legend, the reader is referred to the web version of this article.)

well 2 h after transfection, to obtain a final vitamin D₃ concentration of 500 nM. Twenty four hours post-treatment, cells were lysed with 50 µL of the passive lysis buffer provided in the Dual-Luciferase[®] Reporter (DLR[™]) Assay System kit (Promega) and 10 µL of lysate were transferred to a 96-well plate. Luciferase activity was measured with the substrates LAR II and Stop & Glo[®], also included in the kit, using a GloMax-Multi detection system (Promega). Values obtained for firefly luciferase activity were normalized to renilla's activity, as well as empty vectors such as pGL3-basic or pcDNA3.1. In each experiment, tested conditions were performed in triplicate.

2.10. Electrophoretic mobility shift assay

Electrophoretic Mobility Shift Assay (EMSA) oligos were designed based on *in silico* predicted VDREs, with added 5'-AGCT (fwd) or 5'-GATC (rev) overhangs to allow for their radioactive filling-in reactions, as described previously [19] and indicated in Table 2. They were annealed and subsequently labeled with [³²P]-dATP, using Multiscribe reverse transcriptase (Life Technologies). Nuclear extracts from Caco-2 cells at 70–80% confluence were quantified with the Pierce[™] BCA Protein Assay Kit (Thermo Scientific). Appropriate binding reactions were performed using NE-PER kit (ThermoScientific) and carried out as described [19]. The oligonucleotide named VDREcon, carrying the VDRE consensus sequence AGGTCA in a DR3 repeat, was used as positive control in EMSA. In competition EMSA, unlabeled VDREcon was employed at 100 ng (Cold VDREcon_1) and 200 ng (Cold VDREcon_2), to compete with 150 ng of the labeled oligos for the VDR.

2.11. Statistical analysis

Gene ontology (GO) and Network analysis of the next-generation sequencing data were performed with the MetaCore online software (Thomson Reuters). Dual-luciferase assay data were analyzed with One-way analysis of variance followed by Dunnett's *post-hoc* test, using GraphPad 5.0. Error bars represent the standard error of the mean values from at least 3 experiments. Differences between treatment and controls (*) were considered significant when $p \leq 0.05$.

3. Results

3.1. Global effects of Vitamin D₃ in Caco-2 cells: next generation sequencing (NGS)

Vitamin D₃ plays an important role in the regulation of several SLC transporters and metabolizing enzymes. Caco-2 cells were treated with vitamin D₃ for 24 h and total RNA was extracted and analyzed by NGS. Changes in gene expression were considered significant when p value ≤ 0.05 and expression was at least 41% increased (\log_2 ratio ≥ 0.5) or decreased (\log_2 ratio ≤ -0.75), compared to the vehicle control (EtOH). Consistent with previous reports, vitamin D₃ increased expression of genes implicated in its own catabolism, namely, CYP24A1 and CYP3A4, as well as genes involved in calcium homeostasis, such as the calcium channel TRPV6, implicated in intestinal calcium absorption. The acknowledged mechanism by which these inductions occur is by VDR binding to VDREs in the promoter regions of these genes [4,20–22]. Of all 208 upregulated and 352 downregulated genes significantly affected (Fig. 1), vitamin D₃ 24-hydroxylase CYP24A1 showed the strongest change in expression, with an increase of above 1000-fold and was followed by the calcium channel TRPV6, with over 100-fold increase (\log_2 ratio_(24h) = 6.989; p -value = $5.37e^{-56}$). Also consistent with previous reports [23], vitamin D₃ increased expression of the cytosolic sulfotransferase SULT1C2. The UDP

glycosyltransferase UGT1A1 and the retinoic acid hydroxylase and CYP26A1 were among the relevant metabolizing enzymes whose expression was augmented by vitamin D₃ (Table 1).

NGS data endorsed our previous observations that vitamin D₃ transactivates the organic anion transporting polypeptide 1A2 (OATP1A2; SLC01A2 gene) and the proton-coupled folate transporter (PCFT; SLC46A1 gene) [6,24]. Here, their expression levels increased by approximately 2-fold each (Table 2). Vitamin D₃ also enhanced expression of nutrient transporters such as the fatty acid transport protein (FATP2; SLC27A2) and the carnitine/acylcarnitine carrier (CAC; SLC25A20). In contrast, expression of genes encoding the organic anion transporter 4 (OAT4; SLC22A11) and the glucose transporter 2 (GLUT2; SLC2A2) was considerably reduced. In addition to the OATP1A2, PCFT and OAT4, which transport

Table 1

Gene expression of metabolizing enzymes significantly affected by Vit. D treatment in Caco-2 cells for 24 h. Gene expression levels are quantified as \log_2 ratio of treatment (vitamin D₃) vs. control (EtOH) and converted with $2^{(\log_2 \text{ratio})}$ to denote fold change: 0.5 corresponds to 1.41 fold change, i.e., 41% increase in gene expression.

Increased Metabolizing Enzymes			
Gene	Fold change	log ₂ Ratio	p Value
CYP24A1	1184.45	10.21	0
UGT1A1	5.34	2.418	1.22E-10
SULT1C2	5.34	2.417	2.11E-35
CYP3A4	3.64	1.863	0.0008559
CYP26A1	2.75	1.462	0.01259
CYP2S1	2.25	1.168	3.47E-81
NAT8B	1.69	0.7585	0.02615
NAT8	1.65	0.722	0.02123
CYP3A5	1.64	0.7173	5.54E-33
CYP1A1	1.58	0.656	3.79E-15
CYP2C19	1.53	0.6158	0.04933
Decreased Metabolizing Enzymes			
Gene	Fold change	log ₂ Ratio	p Value
CYP4B1	0.46	-1.124	0.04988
SULT1B1	0.51	-0.9653	0.01921
NAT2	0.56	-0.8267	0.01868
CYP4X1	0.58	-0.7797	0.002375

Table 2

Gene expression of nutrient and drug transporters significantly affected by Vit. D treatment in Caco-2 cells for 24 h. Gene expression levels are quantified as \log_2 ratio of treatment (vitamin D₃) vs. control (EtOH) and converted with $2^{(\log_2 \text{ratio})}$ to denote fold change: 0.5 corresponds to 1.41 fold change, i.e., 41% increase in gene expression.

Increased Transporters				
Gene	Fold change	log ₂ Ratio	pValue	Protein
SLC30A10	15.13	3.919	5.65E-23	ZnT10
SLCO1A2	2.30	1.201	0.0001578	OATP1A2
SLC27A2	2.17	1.121	2.55E-82	FATP2
SLC46A1	2.06	1.042	5.47E-132	PCFT
SLC46A2	2.01	1.007	0.04443	TSCOT
SLC2A9	1.76	0.819	0.00931	GLUT9
ABCC2	1.64	0.714	3.31E-40	MRP2
ABCB1	1.63	0.705	1.02E-27	MDR1/Pgp
SLC1A3	1.51	0.594	1.02E-31	EAAT1
SLC25A20	1.43	0.518	9.84E-17	CAC
Decreased Transporters				
Gene	Fold change	log ₂ Ratio	pValue	Protein
SLC22A11	0.38	-1.403	3.62E-05	OAT4
SLC2A2	0.54	-0.8975	0.005613	GLUT2
SLC39A2	0.56	-0.8417	0.004084	ZIP-2

Table 3

Degree of change in gene expression for selected pathways affected by Vit. D treatment of Caco-2 cells for 24 h.

Vit D 24-hydroxylase activity
CYP24A1 (10.21), CYP3A4 (1.86)
Iron homeostasis
CP (3.30), HP (1.99), SLC46A1 (1.04), FTH1 (0.25), SLC25A37 (0.18), CYBRD1 (−0.24), HFE (−0.26), SLC40A1 (−0.34), EPOR (−0.32), SLC39A2 (−0.84), TTYH1 (−2.14)

CP = ceruloplasmin, HP = haptoglobin, SLC46A1 = PCFT/HCP1, FTH1 = ferritin, HFE = hemochromatosis, SLC40A1 = ferroportin, EPOR = erythropoietin, TTYH1 = tweety family member 1. Numbers in parentheses indicate gene expression levels quantified as Log₂ ratios. When converted with $2^{\text{Log}_2 \text{ratio}}$, they indicate fold changes: (0.5) corresponds to a 1.41 fold, or 41%, change in gene expression.

endogenous as well as drug molecules into the cell, e.g., fexofenadine (OATP1A2), methotrexate (PCFT) and torasemide (OAT4), the efflux transporters multidrug resistance-associated protein 2 (MRP2) and the P-glycoprotein-1 (P-gp) also responded to vitamin D₃ treatment in Caco-2 cells (Table 2).

Network analysis shows iron homeostasis among the top differentially expressed pathways due to vitamin D₃ treatment, alongside with neuropeptide signalling, inflammation, cell adhesion and morphogenesis (Fig. 1D). These results agree with several reports on the putative or confirmed modulatory effects of vitamin D in innate and adaptive immunity, cell growth and differentiation [10,25–27]. Among the genes involved in iron homeostasis, the iron oxidase ceruloplasmin (~10-fold increase), the hemoglobin binding protein haptoglobin (~4-fold increase), and SLC46A1, also known as the heme-iron carrier 1 (HCP1) [28], had the most remarkable increase in gene expression. In contrast, expression of SLC39A2 and the tweety family member 1 (TTYH1) were significantly reduced (Table 3). While TTYH1 is possibly an iron transporter [29], SLC39A2 was shown to play an important role in iron homeostasis in zinc deficient mice [30]. SLC39A2 is part of the ZIP (SLC39) family, implicated in zinc, iron and/or manganese transport [31].

Vitamin D has been shown to have beneficial effects in neurological diseases where neuropeptide, especially glutamate, signaling is dysregulated, such as schizophrenia [32] and Parkinson's disease [33–35]. Our NGS data shows an ~50% increase in the glutamate transporter gene SLC1A3 (Table 2). While genes involved in peptide, amide and sulfur compound binding, glutathione transferase and the major

histocompatibility complex (MHC) class II are downregulated by vitamin D₃ in Caco-2 cells (Fig. 1C), genes involved in enzymatic catalysis, heme and oxygen binding and serine-type endopeptidase activity are upregulated, as revealed by GO analysis (Fig. 1B).

Of all genes that showed increased expression with vitamin D₃ treatment, SLC30A10 was the fourth most strongly affected. It was also the chief affected transporter gene, with ~15-fold increase in expression (Table 2). A concomitant ~45% decrease in expression of the other zinc transporter, SLC39A2, is noteworthy. These zinc transporters work in opposite directions to maintain zinc homeostasis. While members of the ZnT (SLC30) family reduce Zn²⁺ cytoplasmic concentrations via efflux through the plasma membrane or uptake into cytoplasmic organelles, ZIP (SLC39) transporters increase cytoplasmic zinc concentrations by zinc uptake from the extracellular space or efflux from intracellular storage organelles [36]. SLC30A10 is mostly located in the brain, retina, liver and small intestine [7,37], while SLC39A2 has a widespread tissue distribution [38].

3.2. Vitamin D₃ increases SLC30A10 expression in duodenal biopsies and Caco-2 cells: real-time PCR

Real-time PCR validated the NGS observations of strong induction of SLC30A10 by vitamin D₃. Caco-2 cells were treated with 500 nM 1,25 dihydroxyvitamin D₃ (vitamin D₃) or vehicle (EtOH) for 8 h, 24 h, 48 h and 72 h and the effect of vitamin D₃ on SLC30A10 was already observed after 8 h of treatment, while it peaked at 48 h (Fig. 2). This rapid onset, but slow reaching of

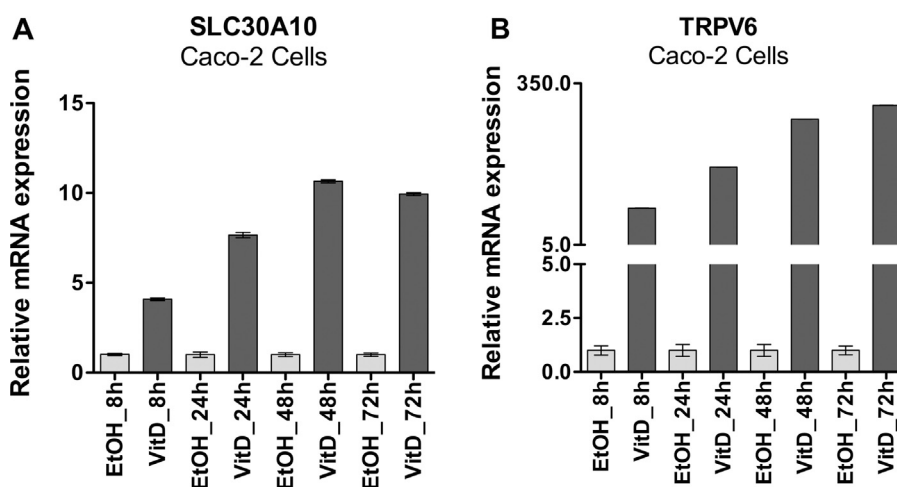


Fig. 2. Vitamin D₃ increases SLC30A10 gene expression time-dependently. Gene expression measured with RT-PCR for SLC30A10 (A) and TRPV6 (B) and normalized to beta actin, from Caco-2 cells treated with 500 nM vitamin D₃ or EtOH, at different time-points.

steady-state may suggest a complex mechanism for SLC30A10 induction by vitamin D₃, possibly with genomic (VDR-mediated regulation of transcription) and non-genomic (activation of signal transduction pathways upon binding to a cell surface receptor) vitamin D₃ modes of action [1]. A strong vitamin D₃ effect was also observed for TRPV6 at all time points. Because TRPV6 is known to have a functional VDRE [4,22] and is highly expressed in the duodenum [39], it was considered a suitable positive control in the RT-PCR measurements in Caco-2 cells, as well as in human duodenal biopsies. Biopsies were collected from healthy human volunteers, before and after oral administration of 0.5 µg 1,25-dihydroxyvitamin D₃ for 10 days. All biopsy-derived mRNA measurements were normalized to villin. TRPV6 induction was noticeable in 70% of the duodenal biopsies, while

SLC30A10 expression was augmented in 60% of the biopsies (Fig. 3).

3.3. Vitamin D₃ increases ZnT10 protein expression in Caco-2 cells: Western blotting and cytofluorescence

Protein expression at the cell surface is critical for the ZnT10 efflux activity and its protective role against Mn toxic accumulation. Mutations in SLC30A10 that result in ZnT10 retention in the endoplasmic reticulum are linked to cases of familial parkinsonism, presenting with Mn accumulation in the liver and the CNS [8,40]. To determine if the vitamin D₃-induced augmentation of SLC30A10 gene expression leads to an increase in ZnT10 protein at the cell surface, we first seeded

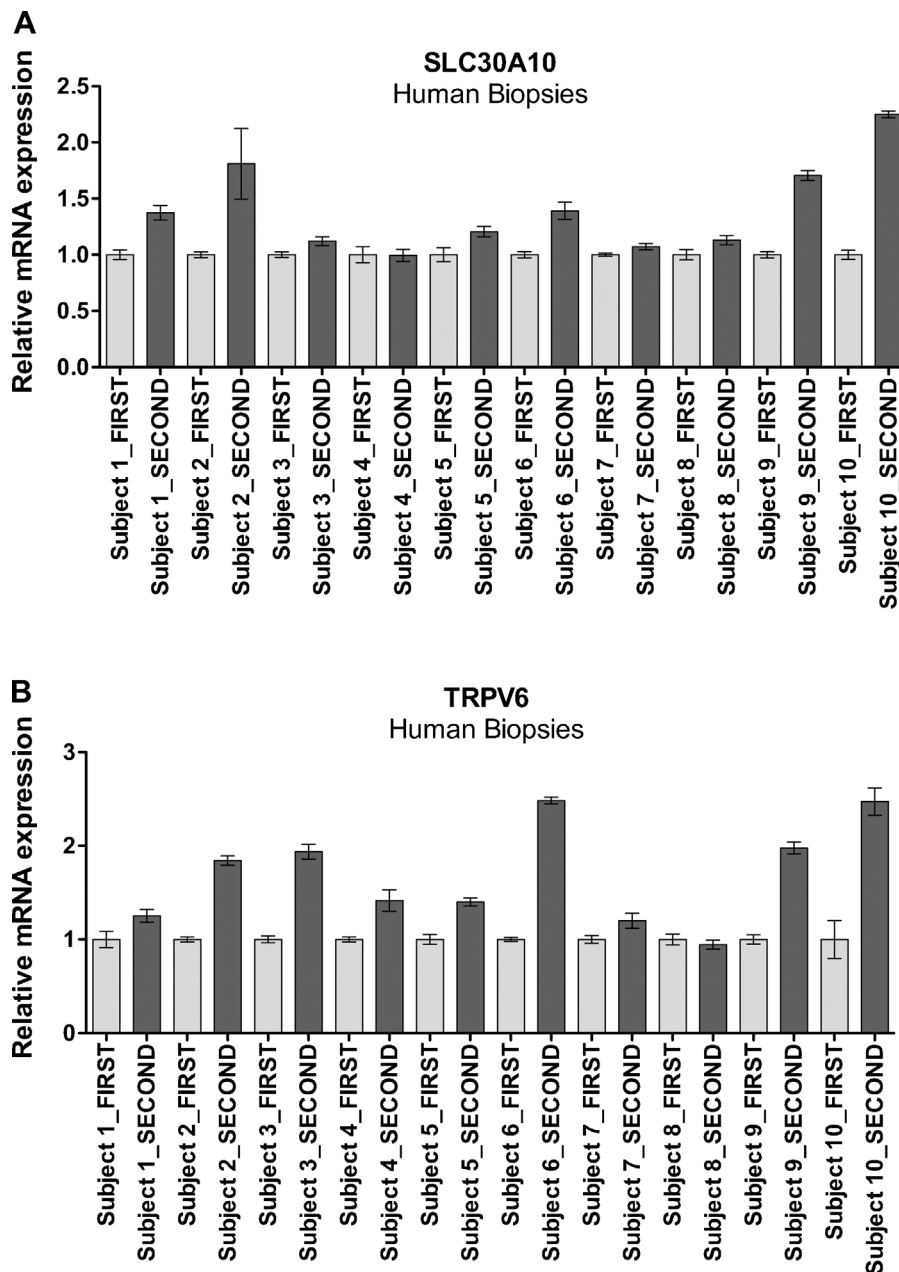


Fig. 3. Vitamin D₃ oral administration increases SLC30A10 and TRPV6 gene expression in duodenal biopsies. RT-PCR of duodenal biopsies collected before (FIRST) and after (SECOND) Rocaltrol[®] 10 days-treatment, in human healthy volunteers. Biopsies were processed as described in methods, Sections 2.3 and 2.4.

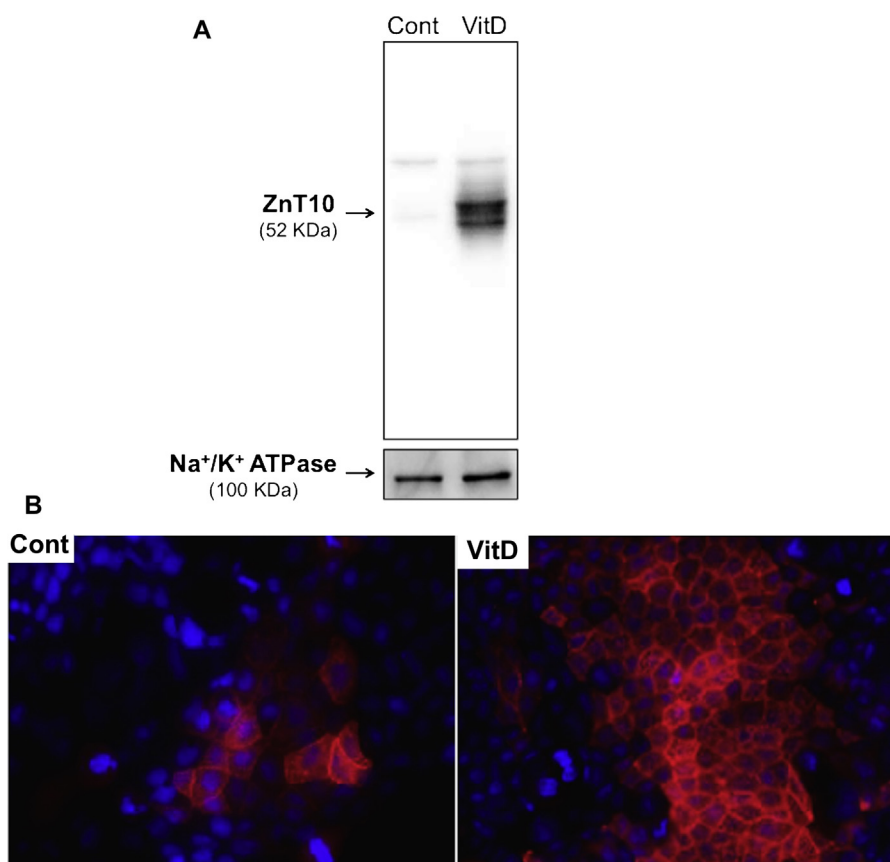


Fig. 4. ZnT10 expression is induced by Vitamin D₃ treatment. A, representative western blot of ZnT10 and the cell surface control Na⁺-K⁺ ATPase, from isolated membrane fractions of Caco-2 cells treated with vehicle (Cont) or Vitamin D₃ (VitD). B, representative staining of Caco-2 cells from vehicle (Cont) or vitamin D₃ (VitD) treatment groups for ZnT10 protein (red). Cells were counterstained with DAPI (blue). (For interpretation of the references to colour in this figure legend, the reader is referred to the web version of this article.)

Caco-2 cells on microscope slides or 10 mm petri dishes and then treated the cells with vitamin D₃ or control (EtOH). We subsequently prepared slides for immunofluorescence detection (Section 2.7) and isolated the membrane fraction of cells grown in the petri dishes (Section 2.5) for Western blotting (Section 2.6), using an anti-SLC30A10 antibody. Vitamin D₃ treatment clearly increased ZnT10 protein levels at the cell surface, as shown by enhanced immunofluorescence along the cell borders in treated cells, compared to control (Fig. 4B). A notable increase in immunoblotting signal for ZnT10, but not the negative control Na⁺/K⁺-ATPase, is also observed in vitamin D₃-treated, but not untreated cells (Fig. 4A). These observations support the hypothesis that vitamin D₃ is important for SLC30A10-mediated Zn and Mn homeostasis.

3.3. Vitamin D₃ activates the SLC30A10 promoter: reporter gene assay

VDR-responsive elements (VDREs) have been found in numerous genes important for calcium homeostasis and vitamin D metabolism, such as TRPV6 and CYP24A1, as well as genes that do not appear to have direct implications in calcium homeostasis, such as SLC01A2 and SLC46A1 [6,24]. These genes respond to vitamin D₃ with an increase in gene expression. Our results show that vitamin D₃ increases SLC30A10 expression at the mRNA and protein levels, prompting us to study whether this is a VDR-mediated effect. We employed the *in silico* prediction tools PROMO [14,15] and MatInspector [16,17], as well as visual inspection [18] and examined the region in the SLC30A10 promoter encompassing

–3622 nucleotides in the 5′-flanking region of the gene, relative to the TSS (position +1), and 211 nucleotides upstream the ATG start codon, *i.e.*, –3622/+211 or ~3.8 kb, using RefSeq NG_032153.1 from the National Center for Biotechnology Information database (Fig. 5A). Because 13 conjectural VDREs were predicted, the DNA sequence corresponding to ~3.8 kb upstream the ATG was used to construct a reporter plasmid in pGL3 basic, as described in Section 2.8 and indicated in the cartoon in Fig. 5B. The resulting construct was tested for promoter activity in a dual-luciferase assay. Classically, heterodimerization of the nuclear VDR with RXR is necessary for VDR-dependent induction to occur. After cotransfecting Caco-2 cells with VDR-pCMX and RXR-pCMX, or with the negative control vector pcDNA3.1, the SLC30A10 promoter construct was incubated with vitamin D₃ or vehicle (EtOH). As shown in Fig. 5B, luciferase activity increased significantly in the presence of VDR, RXR and vitamin D₃, but not with either transcription factor alone or when vitamin D₃ was replaced with EtOH. This observation indicates that the SLC30A10 promoter is transcriptionally activated by vitamin D₃ and that VDR and RXR are required to confer this induction.

3.4. VDR binds to the SLC30A10 promoter region: electrophoretic mobility shift assay

After showing that the 5′-flanking region of the SLC30A10 gene is activated by vitamin D₃ in reporter gene assays and may contain a functional VDRE, we aimed to identify the VDRE or VDREs responsible for this effect. Based on the *in silico* predicted VDRE

A

AGGAGCAGTGGCTCACGCCCATCTCCACTAAAAATACAAAAATTAGCTGGGCGTGGTGGCAGGTGCCTATAATCCCAGCTACTTAGGAGGCTGAGTC
TGGAGAACTGCTTGAACCTGGGAGGTGGAGTGTGCAATGAGCTGAGATCACGCTATTGCACCTCCAGCTGGGTGACAAGAGTGGAGCTCCGCTC
AAAAAAGATGATTGAGTTAGTATAATCTGGAAGCAAAGGGTGAAGCTCTAGAGTTTGGATGCCTAGTTCAAGAGCTCAAATCTATCAAT
CATTTACAGCTTGTGTGGTCTTGGGTAAAGTTACTTAAAAATCTCAGGTTCTATCCTATAAAAATAGTACTTATTTTATGGGGCTGTGATGAGGAAGAAATG
AGATGATGCTTATAAACTCTCAGCACAGGGTTGGGCAGAGTAAGAGATCAATAAACAAAAAGCTATTTAAACCTCACAAATTTGCTGTTAAGTATAAAA
TGCTGGCCAGGTGTGGTGGCTCACGCCTATAATACCAGCAGCTTTAAGGAGGTCAGGCGGGCAGATCATTGAGGCCAGGAGTTCGAGACCAGCTTG
GCCAACGTGGTGAACCCCTATCTACTAAAAAGTACAAAAATTAGCAGGGTGTGGTGGTGCACACTTGTAGTCCCAGCTACTCGGGAGGCTGAGGCAG
GAGAACTCAGTTGAACCCAGAGGGCAGAGGTTGTGGTGGCTGAGATTGGGCCACTGCATTTAGCCTGGGTAACAGAGTAGACTCTGTCTTAAAAAA
AATAAAAAATAAAATGCAGCCTGTATTTTATCAATTAACCTTATATACTGTGTGTGTGTGTGTAGTTTTAGTACAAACATTTTCTACAGTGCTTTT
TTGACACCATCTGGCAACACTTACCCTTTCTTAAAGTCAGGAATGGGTCCCCAGGCAGGCTGCCTCTGCCACTCCAGCTCCTCCAGCTTCTCAGCCA
CTGGCTTTATGGTTCATCCACTGCCTCTGGGCAGTGACACAATCTTATCTGCCTTTGGTTAGGAAAAATAATTGGCAATTTGCTCCAGTGATACA
TTTCTGTGATTTAGGTTTCTTTTCTTCTCAGTGGTGAATGACAAAGACATGCAATTAGCAAGGAATGCTTTAGTTTGTCAAGTTTGTCCACCAGGCTTCCC
TCACTTATTTGACTGTTTGTCTTGTCTGTATTAATGTTTCAGAAAGCTTTACAGTTTGAAGACAGTCTAAGCCAGAAACAGCAATGGCTACAGTACT
CTGATAAATCTCTTTTGTCTATTAGAGTGTCTCATCTGTTGTTCAATAGTAATCCATCACACATGTGCTGTAGTATTAATACTATTGACAACAATAA
GAACATTTATTGAGTGTACTGTGTACCAGGCCTATTTTAAAGCATTTCACACATATTAACCTATTAACTCTTCCCTATACTATTATTCCCATTTTA
CACTAGTAAAAATACCGTAGTCTATATCTTCTTACCTCTACATTAATTGATTATTTTTATGTTGATTTTGA AAAAATACTTCCAATGATCAATTTCTCTA
ATTCTCAATAAAGGATATTTTCTGGAGGTGCAAAATTTAATAAGCTCTGAGTTTGGAGGCTTATCTGGTGTAAAGTGGGACTTGGATCAAGGATGC
TTTAGCATGGCTGTATGGACCTCAGAAAATACTGAAAGACAAGGTTATGTTTTACAAGGCTAAGGACAATGAATAGGGCTAGAGGTTAGGATGTTCTCTG
TGGTTGGGGGAGGTTGGGCTTGGAGACAGGGCCTGTCTATGTCACCCAGGCTGGAGTGCAGTGGCACCACCACGACTCACTGCAGTCTCTCGACTCTT
GGGTTCAAGCCTTCTCCCACTT]AGCCTCTCTCAATA GCTGGGACCATAGGCACACACGCCTGGCTAATTTTTTTTATTTTTTTGTAGAGATGGG
GTTTCCCTATATTGCCAGGCTGATCTTGAACCTCTGGGTTCAAGTGATCCTCCCACTCGGTCTTCCAAAATGTTGAAATTACAGGTGTAAGCCACCA
CGCCTGACCTGTGTTTTTTTTTTTGTGTTGTTTTTTGTTGTTTTTGGAAATAAGACATTGTATTCATTCTAAGCCAAAACCTACATGTGTATTTCTCAGG
AATGGTTAAAGTTCAAGGGCTAGGGATGGGGAAGGAGAATAGAGATGACCAGACTGCACCTTCAAATCCTCTATGGGATGAGATAATGAGACAACA
AAAGAAAACAACAAAGAAACCTAGGAGCCAGGCCTCTCAAACCTCCACAGCAGGAAGAGACCAGCAGCAGACACCCTTCTCAAGGGTCCCTTCT
CAGCCTTCCAGAGTCTGGAGACAGTTACCTTCTGGATAAATTTTATTGGAACACAGCCTGTGTCAATAGAAGAGTCTTGGCCAGGTGCAGTGGC
TCACGCCTGTAATCCAGCACTTTGGGAGGCTGAGGTGGGCAGATCACTTGGAGTCAAGGAGTTCGAGACCAGCCTGGCCAACATGGTGAACCCCTGTC
TCTACTAGAAAATACAAAAATAAAAAATTAGCCGGCATGGTGCCTGTAATCCCAGCTACTCTGGAGGCTGAGGCAGGAGAATCGCTTGAATCCGAGA
GGCGGAGGTTGCAGTGAGCCGAGATGGCGCCATTGCCTCCAGCCTGGGCAACAACAACGAACTCTGTCTCAAAAAAAAAGAGTCTTTATTTGG
AATAAACCTTCATGTAGGTCAGTTCGATTTGACTGCGTATCAGGTCATGCTGTCAAGGACAGTGGGGGTGAGTAGAATATTTCTTCAATGAAGAATGA
GACAAGTACACAGAGGAGGTCAGCCCTGGTTTCTTTGGCGGCAAGGGACTTGTGTCTACCACAAAGTAGACCAGCCTTCGAGTGTAGGAGGAGTG
CATGCTTACAGAAAGTGGGGTCTGCTCTCCTGAGGGTGCCTGCGATTACCCAGGGAAGGAAGCCTTGAAGCGGAAGATCCTGAAGGGGAACGGGGA
CGATCTTGTGCCATGAGTGGGTAATAGGAACGATCCTGCACCGTTTATAATGGCTGTGAGGAACAAGAGAGGATTAATAGCTTTATCCTGGGGTTAG
TGGAAATGAGGGTGGAGGGCTGAGTGGCGGATGAGGTCACATTTACGAAATGAAAAGCAGGAAGCACCCTCAAGGGCAAGTTGCCCAAGCCTGTGC
TCCGGGGCCTGCACCTGATTAATATGGAATCTGCACCGCAAGGTGCCTATGGGCACGTACGCGAAGGTGTCCAGTCCACCCGAGCGAACACACCCC
ACAGCAGCCAAGGCCCTTATGACTGAGTCAACAGGACACTGGCGACCCCTGAGGGCCAGGAGAAGCGGGGTGTCTGGGTGAATCCCACCTCTGCATGG
GGAGGAGTCTGTGAAGATTGACGTCCAGACACGCCCCCTCTCCTCCGACGCGCCCTCTCTGCACAGTCTGTCCCACAAAAGAGAGACATCGGCTCG
TGGCCACCTGCCAAGTCAGGCCAGGCCGAGGGAGGGGAAAAGGGCCGCGGGAGGCGGTGCACGGGCTGTTCAAGATACTGCCCCGCCACTCCTT
TAGACTCTGGACGTGCGGGACTGGTGGCGTCTGGCCTCGCGTTAAAAAGCGGTGGGCAGGGCCGCGAGACAATCTGGGAGGCGGTACCGGG
CCTCACGGATCCGCGCCGCCCCACCTGTGGCTGCGCGCGGGTGGCTGCGCTCCCTTGGCGCGCGCGGGCGCCGGGGCTGGTGGCGAGATC
GGCCGCTACTCTGGCAAGACGTGCCGGCTGCTTTCATGCTGGTGTCTACCGTTCGCTTCTTCTGGCGGAGCTGGTCTCCGGCTACCTGGGCACTCC
ATCGCGCTGCTCTCCGACT

Fig. 5. SLC30A10 promoter sequence and reporter gene activity. (A) 5'-flanking region ~3.8 Kb upstream the SLC30A10 gene start codon (ATG). Putative VDREs and the ATG start codon are highlighted in blue and red, respectively, and EMSA oligos are enclosed in boxes. NCBI RefSeq NG_032153.1. (B) SLC30A10 promoter activity measured by dual-luciferase reporter assay. Caco-2 cells were transiently transfected with the SLC30A10 promoter region -3622/+211 (relative to the TSS) in the luciferase reporter vector pGL3 basic. Expression plasmids of the human VDR (pCMX) and/or RXR (pCMX) or empty vector (pCDNA3.1), as well as the transfection efficiency control pHRG-TK Renilla reniformis luciferase reporter plasmid, were co-transfected. Vitamin D₃ or EtOH was added 2 h post-transfection, in a final concentration of 500 nM and incubated for 24 h, after which cells were harvested and luciferase and renilla activities measured. Firefly luciferase values were normalized to renilla's values in each well, and data was normalized to the appropriate empty vectors. Bars represent the standard error of the mean for three independent experiments, each performed in triplicate. Results were analyzed with One-way analysis with Dunnett's *post-hoc* test in GraphPad 5.0b, with differences being considered significant (*) when $p \leq 0.05$.

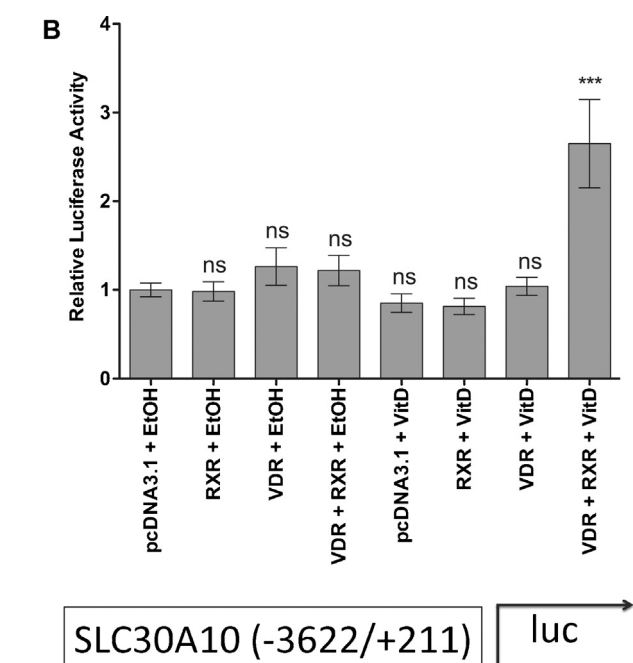


Fig. 5. (Continued)

sequences, we designed oligos with 5'-AGCT (fwd) or 5'-GATC (rev) overhangs, to allow for their radioactive filling-in reactions (Table 4), and tested them in EMSA. As evidenced from the resulting DNA-protein shift (Fig. 6A), nuclear extracts from human-derived Caco-2 cells showed protein binding activity to DNA sequences located at -1623/-1588 (oligo #1), and -1758/-1723 (oligo#2), but not -3367/-3332 (oligo#3), from the transcription start site. As a positive control we used the EMSA probe that we showed previously to correspond to the SLC01A2 VDRE at +202/+216 [6]. We then used a molar excess of cold probe containing a canonical VDRE sequence, namely VDREcon, to compete with radioactively labeled (hot) oligo#1 and oligo#2 for VDR binding (Fig. 6B). Disappearance of the DNA-protein shift band in the presence of competitor confirms that the VDR binds to the SLC30A10 promoter region, at nt -1623/-1588 (oligo #1), and nt -1758/-1723 (oligo#2) relative to the TSS.

4. Discussion

Vitamin D is essential for human health. Its active form, the hormone 1,25-dihydroxyvitamin D (1,25D), or vitamin D₃, has pleiotropic effects beyond calcium homeostasis and bone metabolism. Vitamin D deficiency is associated with increased risk for osteoporosis, cancer, diabetes, multiple sclerosis, hypertension, inflammatory and immunological diseases, among other illnesses [41]. Classically, the vitamin D₃ effects are mediated by the VDR, which in turn is estimated to regulate the expression of

about 500 human genes [1]. Our current NGS results from vitamin D₃-treated Caco-2 cells corroborated previous observations that vitamin D₃ increases expression of the vitamin D hydroxylase CYP24A1, SULT1C2 and SLC01A2 [4,6,20–24] (Table 2), as well as of genes involved in neuropeptide signalling, inflammation, cell adhesion and morphogenesis [10,25–27] (Fig. 1D). In line with the pleiotropic nature of vitamin D₃ effects, we observed alterations in genes with distinct functions, many of which are important for nutrient and drug transport, as well as phase I and phase II metabolism (Tables 1 and 2). Iron and heme metabolism were revealed by network analysis as greatly affected by vitamin D₃ treatment in Caco-2 cells. These observations were further corroborated by GO analysis, where genes involved in oxygen and heme binding were among those affected most by vitamin D₃ treatment (Fig. 1B). While additional experiments would be useful to verify these outcomes *in vivo*, for example, the effect of VDR knockout on iron homeostasis, our current results may provide a preliminary molecular basis for a conceivable link between vitamin D status and iron homeostasis. This link can be inferred from *in vivo* animal studies and clinical human data. For instance, four weeks' administration of high doses of dietary vitamin D₃ to Wistar rats enhanced iron intestinal absorption and hepatic iron stores [42], while, conversely, rats fed an iron deficient diet exhibited decreased serum vitamin D and bone mineral density (BMD) [43]. In a randomized controlled double-blind trial with iron-deficient menstruating women, enhancement of erythropoiesis and iron status was only achieved when skimmed milk was fortified with vitamin D and iron, but not iron alone [44]. Although a direct vitamin D involvement pends confirmation, vitamin D deficiency appears to increase the risk of anemia in healthy female children and adolescents [45]. Iron deficiency has been hypothesized as a risk factor for osteoporosis [46]. Overall, our data support an association between the effects of vitamin D and iron at the molecular level that would warrant further investigation.

Expression of various transporter genes was significantly altered by vitamin D₃ in Caco-2 cells. SLC30A10, encoding the zinc and manganese transporter ZnT10, was the transporter with the highest increase in gene expression, with remarkable increase in protein expression as well, and we hereby show that transactivation by the VDR is responsible, at least partly, for this response. Zinc and manganese are trace elements whose concentrations need to be tightly regulated to prevent the toxic effects of their accumulation in the body. Zinc is required for the activity of several enzymes, including DNA and RNA polymerases, for the immune system and as a structural component of transcription proteins. Among the many pathological consequences of Zn deficiency are growth impairment, dermatitis, diarrhea and neuropsychological diseases [47], whereas surges in its systemic levels correlate with anemia, leukopenia, neutropenia, copper and iron deficiency [48]. Manganese is important for bone development, lipid, carbohydrate and amino acid metabolism [11], but in high concentrations, causes parkinsonism, dystonia, hypermanganesemia, steatosis, cirrhosis and polycythemia [9]. The need to keep these micronutrients at a narrow concentration range is

Table 4

Top strands of oligonucleotides used as EMSA probes, numbered relative to the transcriptional start site of the human SLC30A10 gene (NCBI RefSeq NG_032153.1).

Oligonucleotide	ID	Sequence (5'-3')
SLC30A10(-1623/-1588)fwd	oligo #1	AGCTATCTTGAACCTCTGGGTTCAAGTGATCTCCACCT
SLC30A10(-1758/-1723)fwd	oligo #2	AGCTTCTCGACTTCTGGGTTCAAGCTTCTCCCACTTT
SLC30A10(-3367/-3332)fwd	oligo #3	AGCTGAGTTTGATGCCTAGTTCAGAGCTCAAATCTATCAA
VDRE consensus probe_fwd	VDREcon	AGCTGCAGGGGGAGGTCAAAGAGGTCACACTAGTA
SLC01A2(+202/+216)fwd	OATP1A2	AGCTTCAGAAAGGGAACCTCCCTGACCCCTTGAGCT

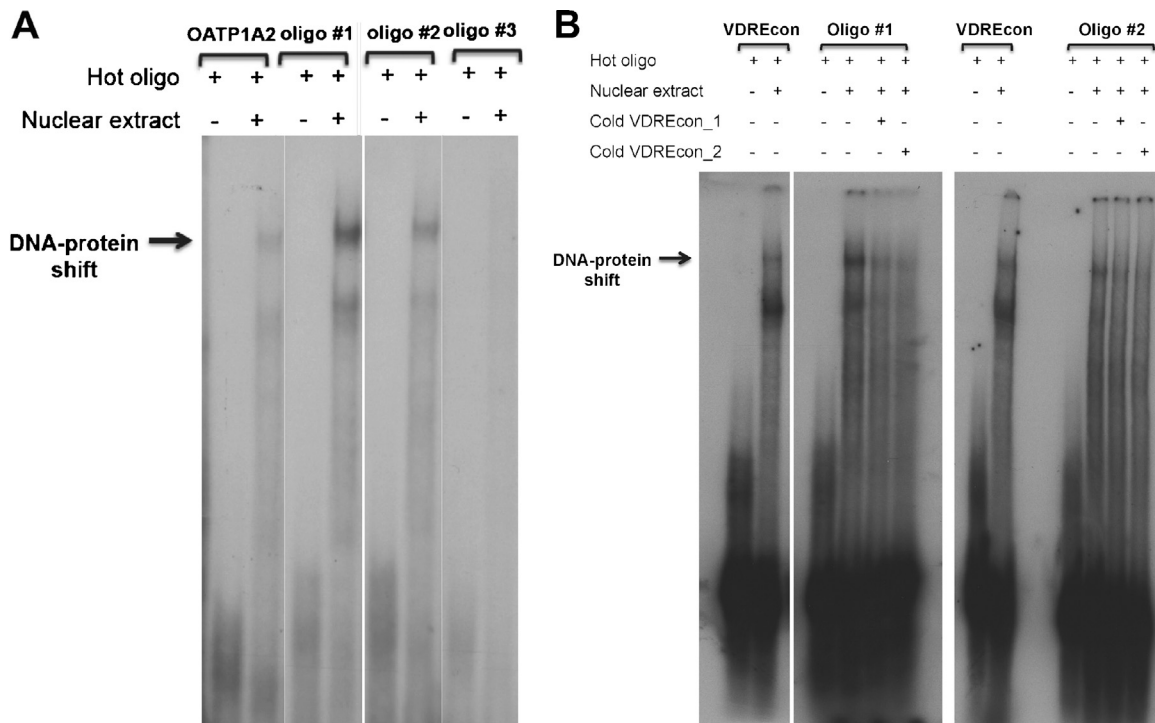


Fig. 6. EMSA showing the VDRE motifs in the SLC30A10 promoter. Double-stranded, radiolabeled oligos at –3367/–3332 (oligo#3), –1623/–1588 (oligo#1) and –1758/–1723 (oligo#2) were co-incubated with binding reaction containing Caco-2 nuclear extract. (A) Only oligos #1 and #2 showed DNA-protein shift bands similar to the positive control OATP1A2 DR3 motif +202/+216. (B) Competition EMSA whereby 200 ng of either radiolabeled oligo#1 or oligo#2 were competed off with cold VDRE consensus probe (VDREcon) using 100 ng (Cold VDREcon_1) or 200 ng (Cold VDREcon_2).

partly accomplished by the strict control of their transport in and out of the cell or intracellular compartments. The metal ion transporter families SLC39 (ZIP) and SLC30 (ZnT) work in opposite directions to ensure zinc and manganese homeostasis. ZIP transporters increase cytoplasmic zinc concentrations *via* zinc uptake from the extracellular environment or efflux from intracellular storage compartments, while ZnT transporters move these ions out of the cell or into intracellular storage organelles, thereby decreasing their cytoplasmic levels [31,36]. There are 10 identified members of the ZnT family: ZnT1–10.

The gene encoding ZnT10, SLC30A10, is chiefly expressed in the liver, brain, testis and small intestine [7,8] and is regulated by zinc *via* a zinc transcriptional regulatory element (ZTRE) [49]. Our results indicate that SLC30A10 expression is modulated by vitamin D₃ *via* the VDR. Upon treatment with vitamin D₃, we observed an increase in SLC30A10 mRNA and protein in Caco-2 cells and in human biopsies, prompting us to investigate a possible involvement of the VDR. The augmentation in SLC30A10 promoter activity strictly in the presence of the VDR, RXR and vitamin D₃ (Fig. 5), as well as EMSA identification of VDREs located in the 5'-flanking region of the SLC30A10 gene (Fig. 6), supported a VDR-mediated transactivation.

In view of the pandemic vitamin D deficiency and widespread supplementation, it would be interesting to understand the physiological and pharmacological implications, if any, of this SLC30A10/ZnT10 induction by vitamin D₃. Theoretically, the ultimate consequence would be a reduction in cytoplasmic levels of Zn and Mn concomitant with a rise in their levels in storage organelles and in the extracellular fluid. It would be tempting to speculate that vitamin D₃ stimulates release of these metal ions into the circulation, to reach organs in need, while aiding vitamin D in some of its physiological actions. For instance, vitamin D₃, Zn and Mn have osteoprotective properties and stimulate bone formation [12]. Zinc has been suggested as an additional

supplement in treatment and prevention of osteoporosis [50] and a possible participation of Mn in the mechanism of osteoporosis has been proposed [51]. It is still unclear whether there is a synergism between vitamin D₃, Zn and Mn, but symptoms of some pathologies may suggest an important link between these nutrients. In inflammatory bowel disease (IBD), celiac disease and food protein-induced gastrointestinal allergy (FPGIA), vitamin D and zinc levels are particularly reduced [52–54]. Although poor absorption is a hallmark of these intestinal diseases, a modulatory effect of these nutrients, whereby imbalance of one nutrient can affect circulating concentrations of the other, cannot be excluded. Associations between childhood wheezing and asthma, when maternal intake of vitamin D and zinc, as well as vitamin E, is inadequate, have also been described [55] and zinc and vitamin D monitoring and supplementation have been suggested as a potential way to control wheezing in children [56].

Mutations in SLC30A10, which prevent ZnT10 expression and function, lead to a toxic accumulation of Mn in the brain, known as manganism. This is a Parkinson-like disease, except patients are not responsive to treatment with L-DOPA or dopamine agonists [57], but instead, to chelation therapy [58]. Hypovitaminosis D is prevalent in patients with early Parkinson's disease (PD) [59,60] and serum 25OHD levels have been shown to correlate with the severity of PD [61]. It would be revealing to examine whether in these patients, hypovitaminosis D would also affect ZnT10 expression or function, and if Mn levels are altered as a consequence.

Our current data corroborates previous reports and brings to light new findings on the molecular role of vitamin D₃ on the homeostasis of iron, manganese and several nutrient/drug transporters, as well as phase I and II enzymes. In particular for zinc and manganese homeostasis, our finding that vitamin D₃ regulates SLC30A10 could trigger future work that assesses a possible role of Zn or Mn supplementation or chelation, alongside vitamin D₃

administration, in the treatment of specific illnesses, such as osteoporosis and PD.

Acknowledgements

Authors thank Dr. Jessica Mwinyi, M.D., M.Sc., Ph.D. for helpful discussions and Dr. Bruno Stieger for expert advice on isolation of membrane fractions for western blotting. This work was supported by grant 320030_144193/1 from the Swiss National Science Foundation.

References

- [1] A.W. Norman, From vitamin D to hormone D: fundamentals of the vitamin D endocrine system essential for good health, *Am. J. Clin. Nutr.* 88 (2) (2008) 491S–499S.
- [2] H. Dobnig, A review of the health consequences of the vitamin D deficiency pandemic, *J. Neurol. Sci.* 311 (1–2) (2011) 15–18.
- [3] M.F. Holick, Vitamin D deficiency, *N. Engl. J. Med.* 357 (3) (2007) 266–281.
- [4] M.B. Meyer, et al., The human transient receptor potential vanilloid type 6 distal promoter contains multiple vitamin D receptor binding sites that mediate activation by 1,25-dihydroxyvitamin D₃ in intestinal cells, *Mol. Endocrinol.* 20 (6) (2006) 1447–1461.
- [5] G. Jones, D.E. Prosser, M. Kaufmann, 25-Hydroxyvitamin D-24-hydroxylase (CYP24A1): its important role in the degradation of vitamin D, *Arch. Biochem. Biophys.* 523 (1) (2012) 9–18.
- [6] J.J. Eloranta, et al., The SLC01A2 gene: encoding human organic anion-transporting polypeptide 1A2, is transactivated by the vitamin D receptor, *Mol. Pharmacol.* 82 (1) (2012) 37–46.
- [7] H.J. Bosomworth, et al., Efflux function: tissue-specific expression and intracellular trafficking of the Zn transporter ZnT10 indicate roles in adult Zn homeostasis, *Metalomics* 4 (8) (2012) 771–779.
- [8] D. Leyva-Illades, et al., SLC30A10 is a cell surface-localized manganese efflux transporter: and parkinsonism-causing mutations block its intracellular trafficking and efflux activity, *J. Neurosci.* 34 (42) (2014) 14079–14095.
- [9] M. Quadri, et al., Mutations in SLC30A10 cause parkinsonism and dystonia with hypermanganesemia: polycythemia, and chronic liver disease, *Am. J. Hum. Genet.* 90 (3) (2012) 467–477.
- [10] C.M. Girgis, et al., Vitamin D signaling regulates proliferation, differentiation, and myotube size in C2C12 skeletal muscle cells, *Endocrinology* 155 (2) (2014) 347–357.
- [11] C.G. Fraga, Relevance, essentiality and toxicity of trace elements in human health, *Mol. Aspects Med.* 26 (4–5) (2005) 235–244.
- [12] I. Zofkova, P. Nemcikova, P. Matucha, Trace elements and bone health, *Clin. Chem. Lab. Med.* 51 (8) (2013) 1555–1561.
- [13] Y. Wang, J. Zhu, H.F. DeLuca, Where is the vitamin D receptor? *Arch. Biochem. Biophys.* 523 (1) (2012) 123–133.
- [14] X. Messegue, et al., PROMO: detection of known transcription regulatory elements using species-tailored searches, *Bioinformatics* 18 (2) (2002) 333–334.
- [15] D. Farre, et al., Identification of patterns in biological sequences at the ALGGEN server: PROMO and MALGEN, *Nucleic Acids Res.* 31 (13) (2003) 3651–3653.
- [16] K. Cartharius, et al., MatInspector and beyond: promoter analysis based on transcription factor binding sites, *Bioinformatics* 21 (13) (2005) 2933–2942.
- [17] K. Quandt, et al., MatInd and MatInspector: new fast and versatile tools for detection of consensus matches in nucleotide sequence data, *Nucleic Acids Res.* 23 (23) (1995) 4878–4884.
- [18] A. Toell, P. Polly, C. Carlberg, All natural DR3-type vitamin D response elements show a similar functionality in vitro, *Biochem. J.* 352 (Pt. 2) (2000) 301–309.
- [19] D. Finke, M.L. Eloranta, L. Ronnblom, Endogenous type I interferon inducers in autoimmune diseases, *Autoimmunity* 42 (4) (2009) 349–352.
- [20] R. Kumar, et al., Systematic characterisation of the rat and human CYP24A1 promoter, *Mol. Cell. Endocrinol.* 325 (1–2) (2010) 46–53.
- [21] Z. Wang, et al., Interplay between vitamin D and the drug metabolizing enzyme CYP3A4, *J. Steroid Biochem. Mol. Biol.* 136 (2013) 54–58.
- [22] J.W. Pike, et al., Molecular actions of 1,25-dihydroxyvitamin D₃ on genes involved in calcium homeostasis, *J. Bone Miner. Res.* 22 (Suppl. 2) (2007) V16–V19.
- [23] E.A. Rondini, et al., Regulation of human cytosolic sulfotransferases 1C2 and 1C3 by nuclear signaling pathways in LS180 colorectal adenocarcinoma cells, *Drug Metab. Dispos.* 42 (3) (2014) 361–368.
- [24] J.J. Eloranta, et al., Vitamin D₃ and its nuclear receptor increase the expression and activity of the human proton-coupled folate transporter, *Mol. Pharmacol.* 76 (5) (2009) 1062–1071.
- [25] R.F. Chun, et al., Impact of vitamin D on immune function: lessons learned from genome-wide analysis, *Front. Physiol.* 5 (2014) 151.
- [26] K. Yin, D.K. Agrawal, Vitamin D and inflammatory diseases, *J. Inflamm. Res.* 7 (2014) 69–87.
- [27] C.M. Girgis, P.A. Baldock, M. Downes, Vitamin D, muscle and bone: integrating effects in development, aging and injury, *Mol. Cell. Endocrinol.* 410 (2015) 3–10.
- [28] S. Le Blanc, M.D. Garrick, M. Arredondo, Heme carrier protein 1 transports heme and is involved in heme-Fe metabolism, *Am. J. Physiol. Cell Physiol.* 302 (12) (2016) C1780–5.
- [29] H.D. Campbell, et al., Human and mouse homologues of the *Drosophila* melanogaster twenty (tty) gene: a novel gene family encoding predicted transmembrane proteins, *Genomics* 68 (1) (2000) 89–92.
- [30] J.L. Peters, et al., Targeting of the mouse Slc39a2 (Zip2) gene reveals highly cell-specific patterns of expression: and unique functions in zinc, iron, and calcium homeostasis, *Genesis* 45 (6) (2007) 339–352.
- [31] D.J. Eide, The SLC39 family of metal ion transporters, *Pflugers Arch.* 447 (5) (2004) 796–800.
- [32] M.V. Wilmsdorff, et al., Gene expression of glutamate transporters SLC1A1: SLC1A3 and SLC1A6 in the cerebellar subregions of elderly schizophrenia patients and effects of antipsychotic treatment, *World J. Biol. Psychiatry* 14 (7) (2013) 490–499.
- [33] K. Vinh Quoc Luong, L. Thi Hoang Nguyen, Vitamin D and Parkinson's disease, *J. Neurosci. Res.* 90 (12) (2012) 2227–2236.
- [34] A. Plaitakis, P. Shashidharan, Glutamate transport and metabolism in dopaminergic neurons of substantia nigra: implications for the pathogenesis of Parkinson's disease, *J. Neurol.* 247 (Suppl. 2) (2000) II25–II35.
- [35] Y. Zhou, N.C. Danbolt, GABA and glutamate transporters in brain, *Front. Endocrinol. (Lausanne)* 4 (2013) 165.
- [36] L. Huang, S. Tapaamorndech, The SLC30 family of zinc transporters – a review of current understanding of their biological and pathophysiological roles, *Mol. Aspects Med.* 34 (2–3) (2013) 548–560.
- [37] S. Sreedharan, et al., Long evolutionary conservation and considerable tissue specificity of several atypical solute carrier transporters, *Gene* 478 (1–2) (2011) 11–18.
- [38] J. Jeong, D.J. Eide, The SLC39 family of zinc transporters, *Mol. Aspects Med.* 34 (2–3) (2013) 612–619.
- [39] J.G. Hoenderop, R.J. Bindels, Calcitropic and magnesiotropic TRP channels, *Physiology (Bethesda)* 23 (2008) 32–40.
- [40] K. Tuschl, et al., Syndrome of hepatic cirrhosis: dystonia, polycythemia, and hypermanganesemia caused by mutations in SLC30A10, a manganese transporter in man, *Am. J. Hum. Genet.* 90 (3) (2012) 457–466.
- [41] M.F. Holick, T.C. Chen, Vitamin D deficiency: a worldwide problem with health consequences, *Am. J. Clin. Nutr.* 87 (4) (2008) 1080S–1086S.
- [42] A.S. Dusso, R.C. Puche, The effect of 1 alpha, 25-dihydroxycholecalciferol on iron metabolism, *Blut* 51 (2) (1985) 103–108.
- [43] S. Katsumata, et al., Severe iron deficiency decreases both bone formation and bone resorption in rats, *J. Nutr.* 139 (2) (2009) 238–243.
- [44] L. Toxqui, et al., Effects of an iron or iron and vitamin D-fortified flavored skim milk on iron metabolism: a randomized controlled double-blind trial in iron-deficient women, *J. Am. Coll. Nutr.* 32 (5) (2016) 312–320.
- [45] J.A. Lee, et al., Low vitamin D levels are associated with both iron deficiency and anemia in children and adolescents, *Pediatr. Hematol. Oncol.* 32 (2) (2016) 99–108.
- [46] L. Toxqui, M.P. Vaquero, Chronic iron deficiency as an emerging risk factor for osteoporosis: a hypothesis, *Nutrients* 7 (4) (2016) 2324–2344.
- [47] M.L. Ackland, A. Michalczyk, Zinc deficiency and its inherited disorders – a review, *Genes Nutr.* 1 (1) (2006) 41–49.
- [48] J. Nriagu, Zinc Toxicity in Humans, Elsevier B.V.: Elsevier Science extranet, 2007, pp. 7.
- [49] L.J. Coneyworth, et al., Identification of the human zinc transcriptional regulatory element (ZTRE): a palindromic protein-binding DNA sequence responsible for zinc-induced transcriptional repression, *J. Biol. Chem.* 287 (43) (2012) 36567–36581.
- [50] M. Yamaguchi, Role of nutritional zinc in the prevention of osteoporosis, *Mol. Cell. Biochem.* 338 (1–2) (2010) 241–254.
- [51] T. Landete-Castillejos, et al., Alternative hypothesis for the origin of osteoporosis: the role of Mn, *Front. Biosci. (Elite Ed.)* 4 (2012) 1385–1390.
- [52] N.R. Santucci, et al., Vitamin and zinc status pretreatment and posttreatment in patients with inflammatory bowel disease, *J. Pediatr. Gastroenterol. Nutr.* 59 (4) (2014) 455–457.
- [53] A.S. Oxentenko, J.A. Murray, Celiac disease: ten things that every gastroenterologist should know, *Clin. Gastroenterol. Hepatol.* 13 (8) (2015) 1387–1552.
- [54] R. Meyer, et al., Dietary elimination of children with food protein induced gastrointestinal allergy – micronutrient adequacy with and without a hypoallergenic formula? *Clin. Transl. Allergy* 4 (1) (2014) p31.
- [55] K. Allan, G. Devereux, Diet and asthma: nutrition implications from prevention to treatment, *J. Am. Diet. Assoc.* 111 (2) (2011) 258–268.
- [56] M. Uysalol, et al., Serum level of vitamin D and trace elements in children with recurrent wheezing: a cross-sectional study, *BMC Pediatr.* 14 (2014) 270.
- [57] J.A. Roth, Correlation between the biochemical pathways altered by mutated parkinson-related genes and chronic exposure to manganese, *Neurotoxicology* 44 (2014) 314–325.
- [58] M. Stamelou, et al., Dystonia with brain manganese accumulation resulting from SLC30A10 mutations: a new treatable disorder, *Mov. Disord.* 27 (10) (2012) 1317–1322.
- [59] M.L. Evatt, et al., Prevalence of vitamin d insufficiency in patients with Parkinson disease and Alzheimer disease, *Arch. Neurol.* 65 (10) (2008) 1348–1352.
- [60] K. vinh quốc Luong, L. Thi Hoàng Nguyễn, Vitamin D and parkinson's disease, *J. Neurosci. Res.* 90 (12) (2012) 2227–2236.
- [61] M. Suzuki, et al., 25-Hydroxyvitamin D, vitamin D receptor gene polymorphisms, and severity of Parkinson's disease, *Mov. Disord.* 27 (2) (2012) 264–271.